

Nanoconfinement-engineered SnPS₃ anodes induced fast electrochemical kinetics for highly reversible sodium-ion storage

Qing Li^a, Weiping Guo^d, Binqiang Chai^d, Kang Xu^b, Weijiang Hu^b, Xueming Su^b, Huaixin Wei^{a*}, Hongbo Geng^{b*}, Jun Yang^{c*}, Zhongzhen Luo^{d*}

^aSchool of Chemistry and life Sciences, Suzhou University of Science and Technology, Suzhou 215009, China.

^bSchool of Materials Engineering, Suzhou University of Technology, Changshu 215500, China.

^cSchool of Material Science and Engineering, Jiangsu University of Science and Technology, Zhenjiang, 212003, China.

^dCollege of Materials Science and Engineering, Fuzhou University, Fuzhou, 350108, China.

Corresponding authors: hxwei@usts.edu.cn; hbgeng@szut.edu.cn; iamjyang@just.edu.cn; zzluo@fzu.edu.cn

Experimental Section

Material characterization

The crystal phase structures of SnPS₃@CNFs and other comparative materials were analyzed by X-ray diffraction (D/MAX-2200/0.15406 K α). The surface properties, relative contents, elemental compositions, and valence states of the samples were investigated by X-ray photoelectron spectroscopy (XPS) using an ESCALAB250 instrument. A Hitachi Regulus 8100 instrument was used for field emission scanning electron microscopy (SEM), a Talos F200X G2 instrument for field emission transmission electron microscopy (TEM), and an FEI Tecnai G2F20 instrument for high-resolution transmission electron microscopy (HR-TEM) to analyze the microstructural characteristics. To supplement these findings, we conducted energy-dispersive spectroscopy (EDS) studies.

Electrochemical measurements

The active material $\text{SnPS}_3\text{@CNFs}$ or relevant control samples, conductive carbon black, and polyvinylidene fluoride were mixed in an exact mass ratio of 7:2:1. Meanwhile, the necessary amount of N-methylpyrrolidone (NMP) was added, and the mixture was carefully ground. To obtain a viscous slurry, the mixture was stirred at ambient temperature for 24 h. Then, the obtained slurry was uniformly coated on a copper foil with a mass loading of 1 - 1.5 mg cm^{-2} , and vacuum-dried at 80 °C for 12 hours. The dried copper foil was manually cut into circular pieces with a diameter of 12 mm, which were used as electrode sheets. The preparation process of NVP cathode is similar to this. NVP, conductive carbon black, and PVDF were mixed at a mass ratio of 7:2:1. Meanwhile, an appropriate amount of NMP was added, and the mixture was carefully ground. To obtain a viscous slurry, the mixture was stirred at room temperature for 24 hours. Subsequently, the resulting slurry was uniformly coated on an aluminum foil and vacuum-dried at 80 °C for 12 hours. The dried aluminum foil was manually cut into circular pieces with a diameter of 12 mm, which served as the NVP cathode sheets. In the CR2032 coin-type half-cell structure, the prepared 12 mm-diameter $\text{SnPS}_3\text{@CNFs}$ electrode sheet was used as the working electrode, and a glass fiber was used as the separator. A sodium disk was used as the counter electrode, and a solution of 1,2-dimethoxyethane (DME) was mixed with 1.0 M NaPF_6 as the electrolyte. In addition, the electrolyte content of all cells was 150 μL . The assembly of sodium-ion batteries was carried out in an Ar-filled glove box, and the contents of water vapor and oxygen were maintained below 0.01 parts per million. The galvanostatic charge-discharge (GCD) tests, along with corresponding rate performance tests and long - cycle performance tests, were conducted using a Neware battery testing system (BTS2300) at room temperature (25 °C) within a voltage range of 0.01 V to 3.00 V. Additionally, cyclic voltammetry (CV) tests were carried out using a CHI660E electrochemical workstation. Electrochemical impedance spectroscopy (EIS) tests were employed to obtain dynamic information inside the anode material. Moreover, the galvanostatic intermittent titration technique (GITT)

tests were used to study the ion diffusion and kinetics during the charge - discharge operations. To assemble a coin - type full cell, the anode sheet was first assembled into a half - cell. Then, this half - cell was cycled for 10 cycles at a current density of 0.1 A g^{-1} for pre - treatment. The separator and electrolyte were made of a glass fiber membrane and 1.0 M NaPF_6 (dissolved in DME = 100 vol%), respectively. The anode and cathode sheets were assembled with other accessories to obtain the full cell. The weight loadings of $\text{Na}_3\text{V}_2(\text{PO}_4)_3$ and $\text{SnPS}_3@\text{CNFs}$ were approximately $3.0 - 5.0 \text{ mg cm}^{-2}$, with a weight ratio of 1:4 (anode:cathode). The full energy density of the battery was calculated based on the total mass of the anode and cathode electrodes.

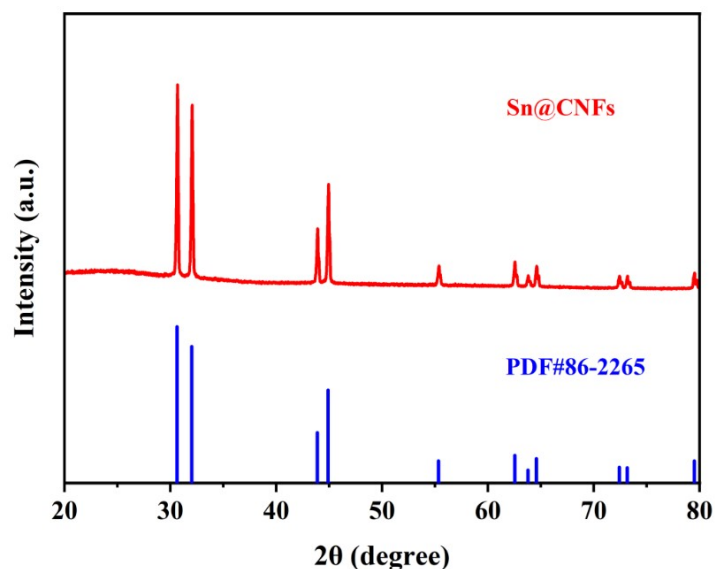


Figure S1. XRD pattern of Sn@CNFs

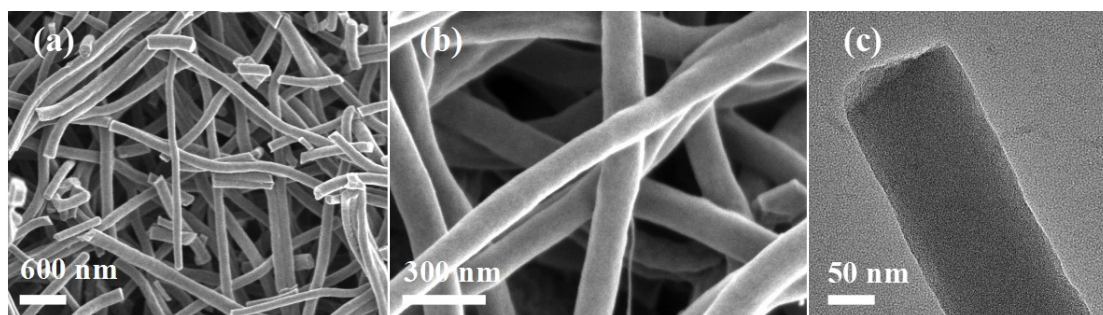


Figure S2. (a-b) SEM images. (c) TEM image of Sn@CNFs .

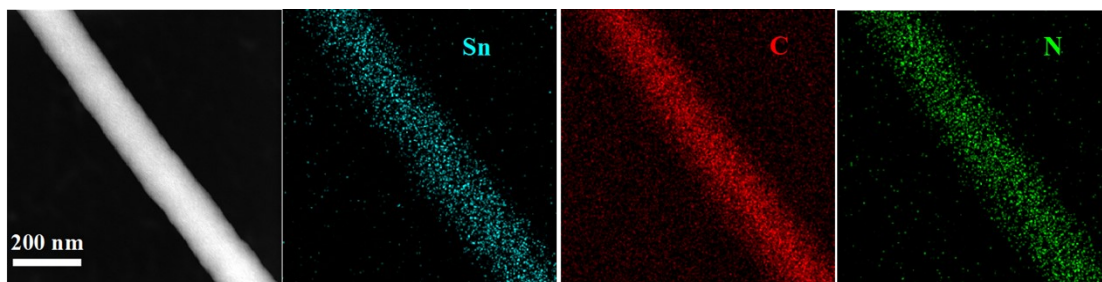


Figure S3. Corresponding elemental mapping images of Sn@CNFs.

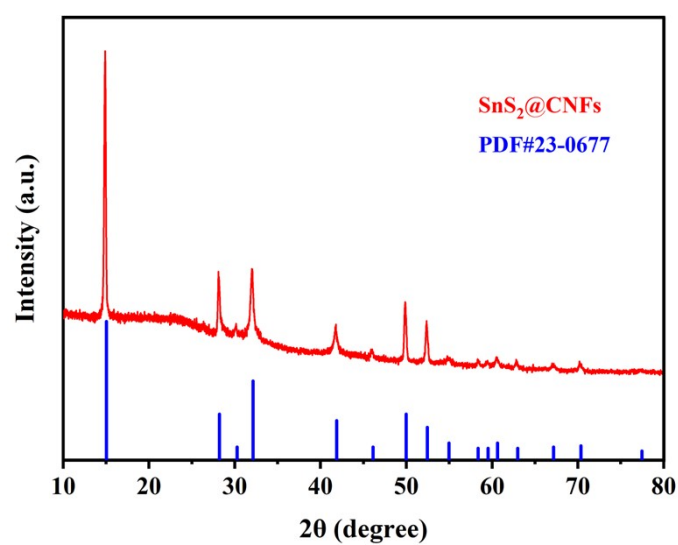


Figure S4. XRD pattern of SnS₂@CNFs.

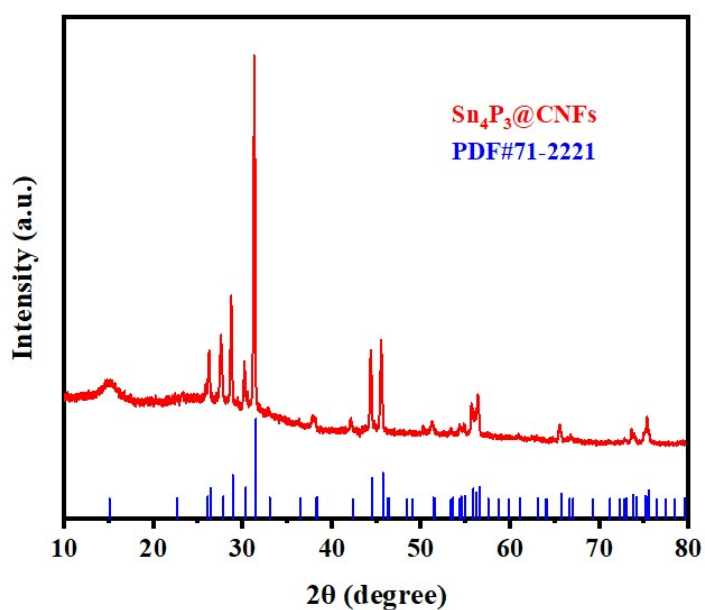


Figure S5. XRD pattern of Sn₄P₃@CNFs.

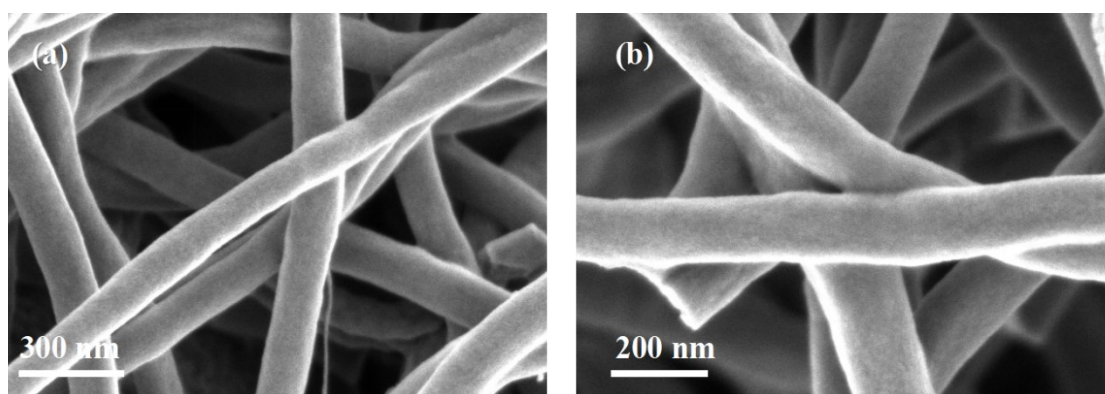


Figure S6. (a-b) SEM images of CNF.

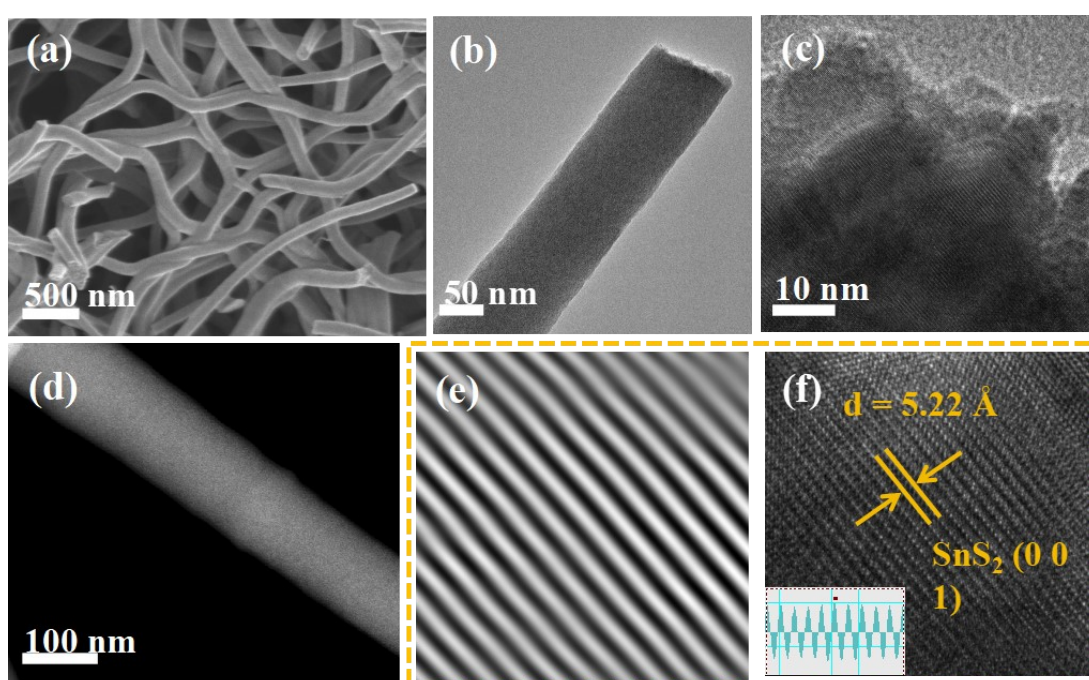


Figure S7. (a) SEM images. (b) TEM image. (c, e-f) HRTEM image of SnS_2 @CNFs.

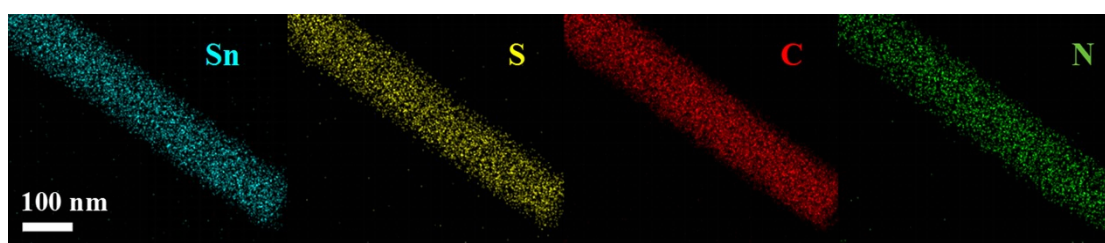


Figure S8. Corresponding elemental mapping images of SnS_2 @CNFs.

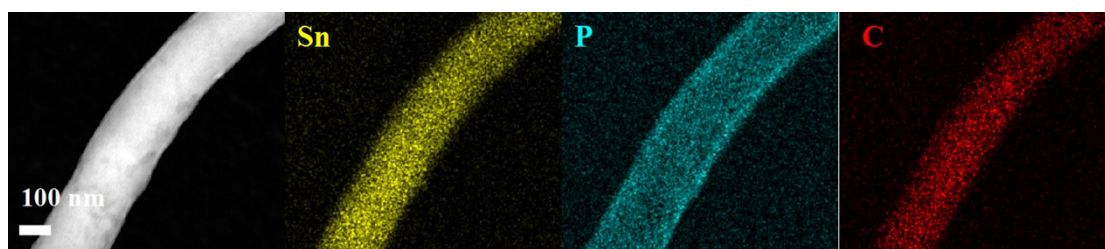


Figure S9. Corresponding elemental mapping images of Sn_4P_3 @CNFs.

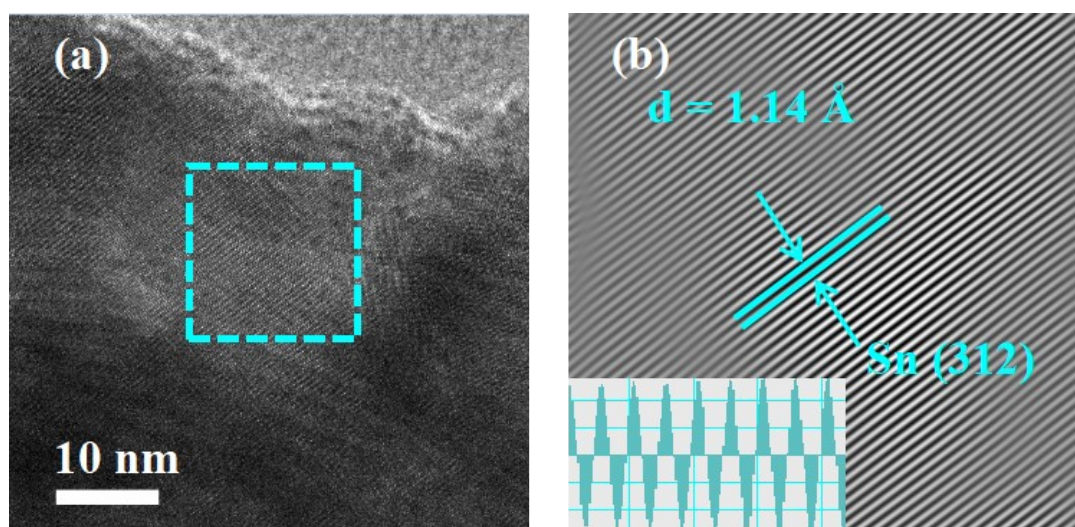


Figure S10. (a-b) HRTEM images of Sn @CNFs

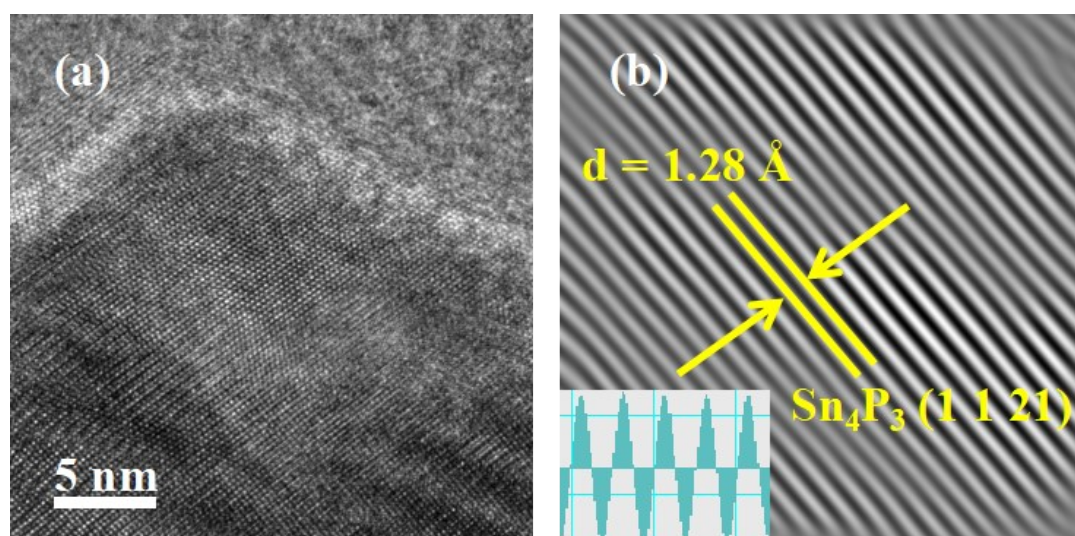


Figure S11. (a-b) HRTEM images of Sn_4P_3 @CNFs

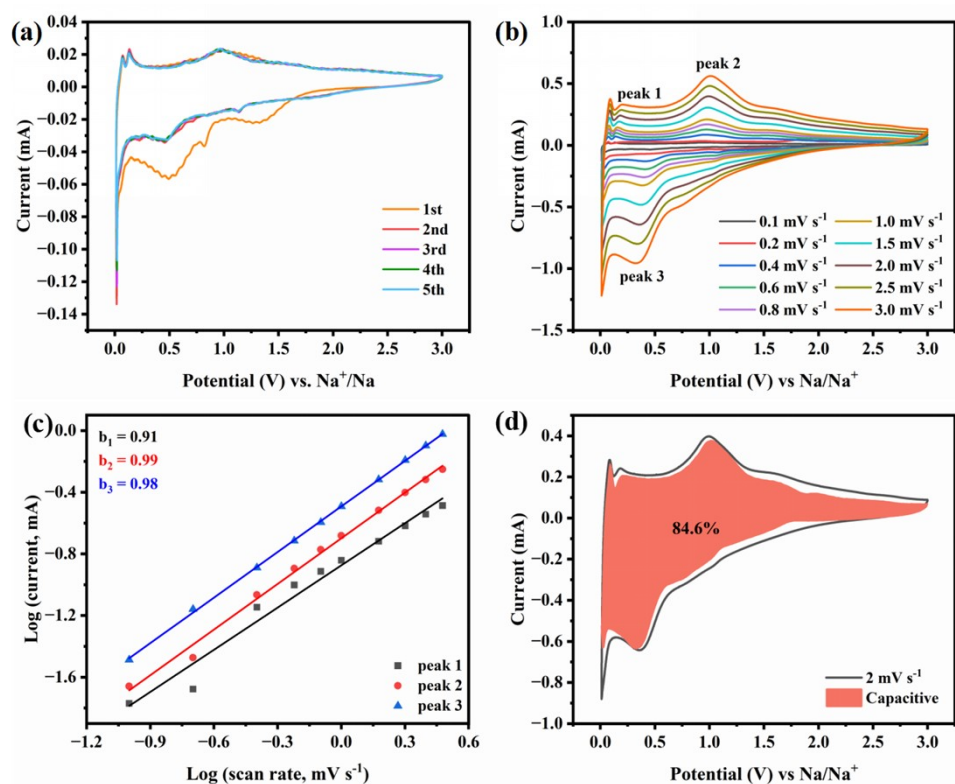


Figure S12. Electrochemical performance of the SnS₂@CNFs electrode. (a) CV curves at 0.1 mV s⁻¹. (b) CV curves. (c) Corresponding log *i* versus log *v* plots. (d) Capacitive contribution.

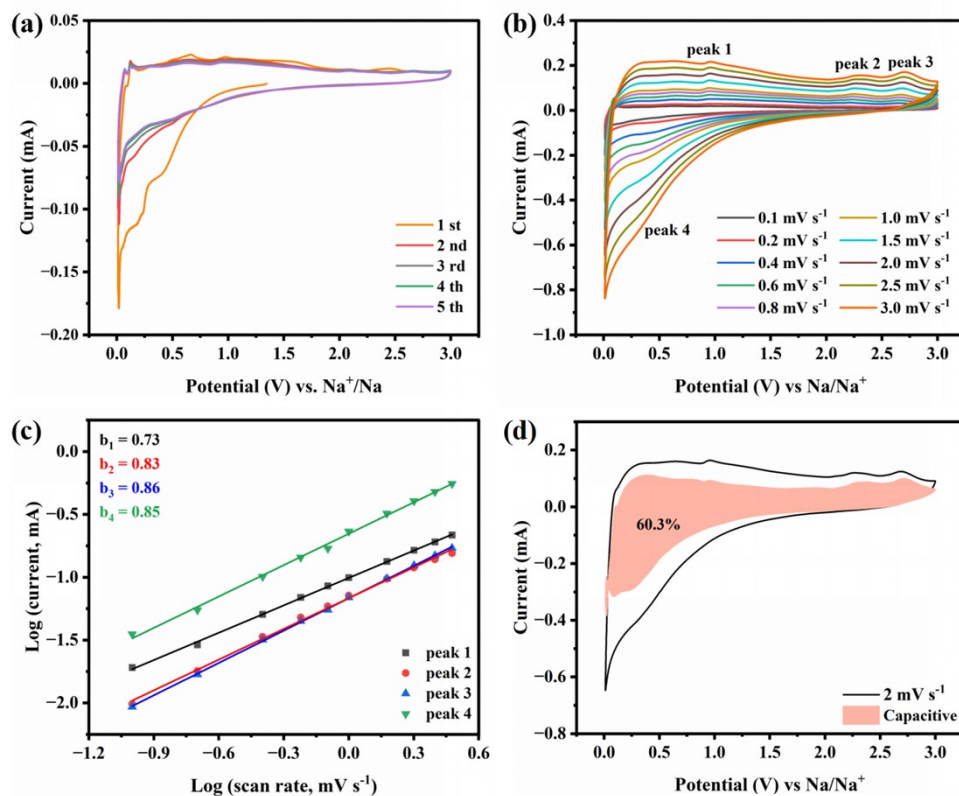


Figure S13. Electrochemical performance of the $\text{Sn}_4\text{P}_3@\text{CNFs}$ electrode. (a) CV curves at 0.1 mV s^{-1} . (b) CV curves. (c) Corresponding $\log i$ versus $\log v$ plots. (d) Capacitive contribution.

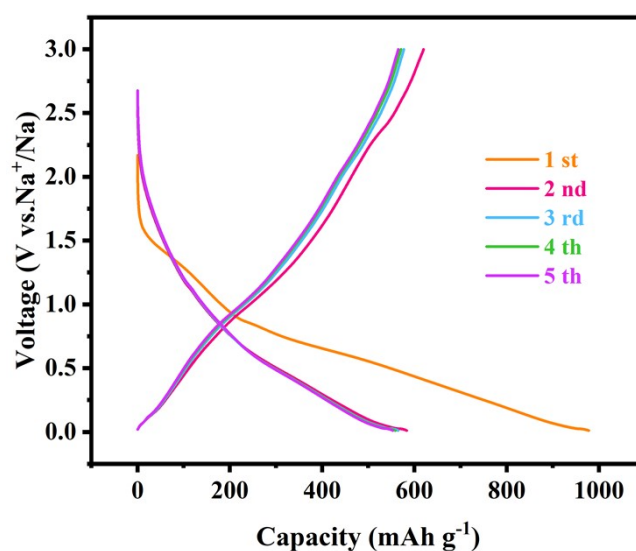


Figure S14. Charge/discharge voltage profiles at 0.1 A g^{-1} of the $\text{SnS}_2@\text{CNFs}$.

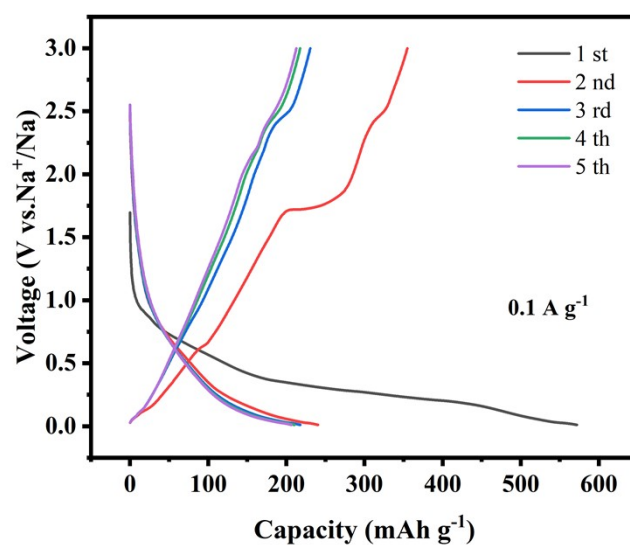


Figure S15. Charge/discharge voltage profiles at 0.1 A g^{-1} of the $\text{Sn}_4\text{P}_3@\text{CNFs}$.

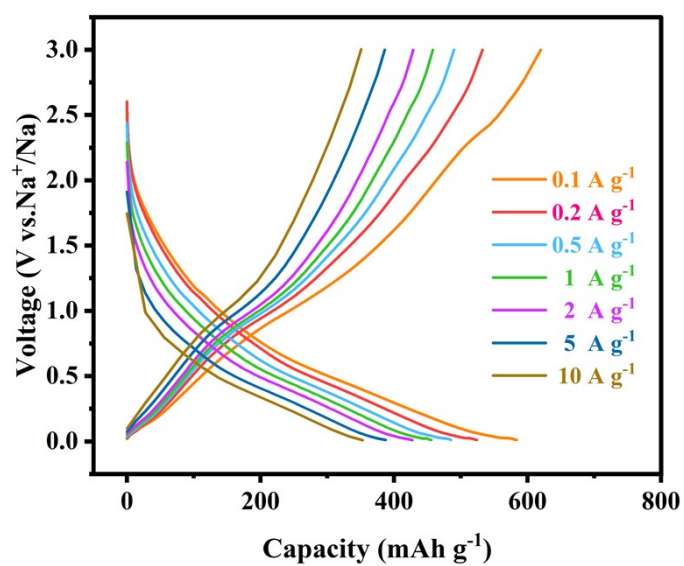


Figure S16. Charge/discharge curves of $\text{SnS}_2@\text{CNFs}$ at various current densities from 0.1 to 10 A g^{-1} .

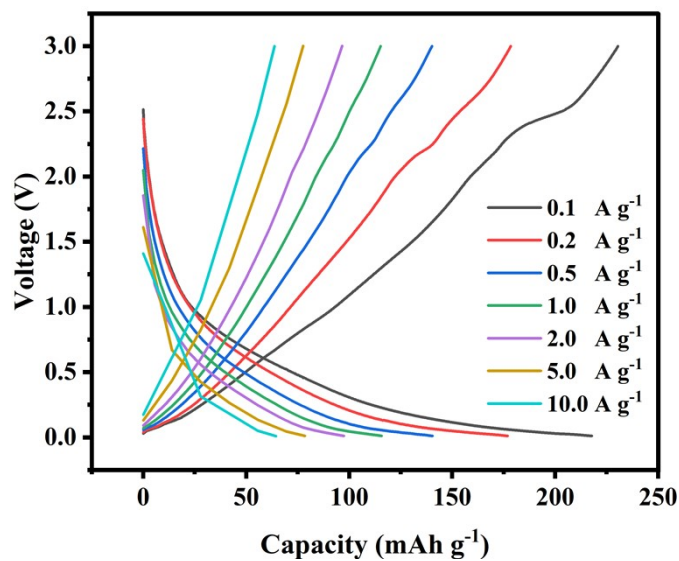


Figure S17. Charge/discharge curves of $\text{Sn}_4\text{P}_3@\text{CNFs}$ at various current densities from 0.1 to 10 A g^{-1} .

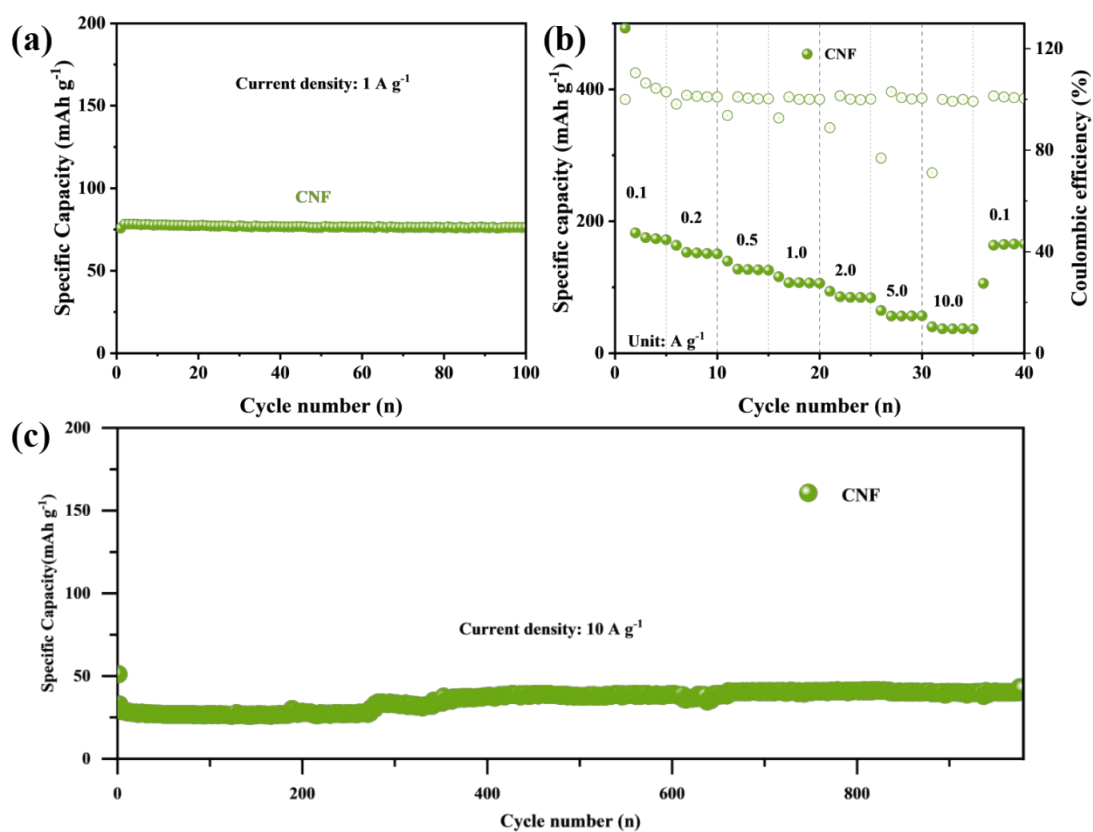


Figure S18. The electrochemical performance of CNF electrode material. (a) Cycle performance at 1 A g^{-1} . (b) Rate performance. (c) Long cycling stability at 10 A g^{-1} .

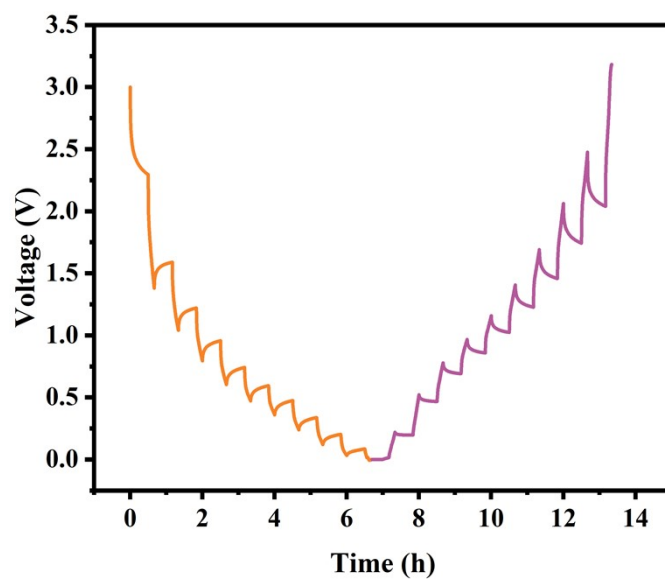


Figure S19. GITT curves of SnS₂@CNFs.

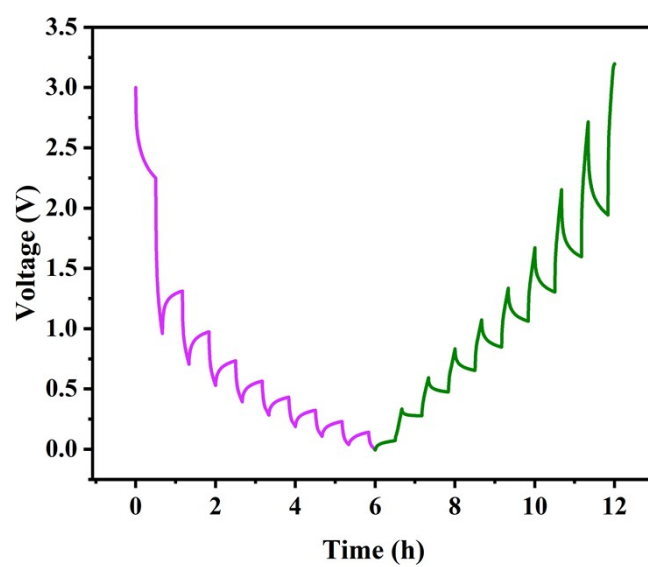


Figure S20. GITT curves of Sn₄S₃@CNFs.